Two-Fluid Toroidal Steady States with Flow

Nathaniel M. Ferraro, Stephen C. Jardin, Andrew C. Bauer

Princeton Plasma Physics Laboratory

CEMM Meeting

Orlando, FL   November 11, 2007

Overview

- Introduction/Motivation
- M3D-C^1
  - Description
  - Progress Since Last Year
  - Implicitization Issues
- Results
  - Testing gyroviscosity with MRI
  - Large-Aspect Ratio
  - NSTX
- Future Directions

Introduction/Motivation

PPPL
PRINCETON PLASMA PHYSICS LABORATORY

- We are trying to calcuate self-consistent, axisymmetric, toroidal steady-states of a comprehensive, two-fluid model.
- In particular, we would like to understand the effects of two-fluid terms and gyroviscosity on the the steady-states.
- Our method is to initialize M3D-C^1, with an ideal-MHD equilibrium, and time-integrate the nonlinear extended-MHD equations until steady state is reached.

Advantages of this Method

Some advantages of integrating the nonlinear physical equations to obtain the steady state:

- Physical coordinates elimiate singularities at separatrix and magnetic axis;
- Fully two-dimensional, allowing general treatments of flow, shape, etc.;
- Plasma core and vacuum region are treated self-consistently;
- Steady state is steady on all timescales;
- Formulation can be straightforwardly extended to more complete physical models and three-dimensions.

M3D-C^1: Overview

- Magnetosonic, shear Alfvén, and whistler waves are all treated implicitly [1].
- Uses a fifth-order C^1 finite-element [2] on a fully unstructured mesh.
- Matrix equations are efficiently and accurately inverted directly using SuperLU_dist [3]. This is made possible by the compactness of the element (asymptotically 3 unknowns per triangle).
- Full axisymmetric two-fluid equations are implemented in both slab and toroidal geometry, including ion gyroviscosity. These equations are essentially the Braginskii equations [4], minus terms proportional to m_e/m_i.
- In the X-MHD equations using flux/potential field representation, no field is differentiated more than four times, with the exception of the hyper-viscous terms. This makes C^1 elements ideal.

M3D-C^1: Physical Model

$$
\begin{aligned}
\frac{\partial n}{\partial t} + \nabla \cdot n\mathbf{u} &= D, \\
n\left(\frac{\partial \mathbf{u}}{\partial t} + \mathbf{u}\cdot\nabla\mathbf{u}\right) &= \mathbf{J}\times\mathbf{B} - (\nabla p + \nabla\cdot\Pi) + \mathbf{R} + \mathbf{F} - \mathbf{u}D, \\
\frac{1}{\Gamma - 1}\left(\frac{\partial p}{\partial t} + \nabla\cdot p\mathbf{u}\right) &= -p\nabla\cdot\mathbf{u} + \frac{d_i}{\Gamma - 1}\frac{\mathbf{J}}{n}\cdot\left(\nabla p_e - \Gamma\frac{p_e}{n}\nabla n\right) \\
&\quad - \nabla\cdot\mathbf{q} - \Pi : \nabla\mathbf{u} + d_i\Pi_e : \nabla\frac{\mathbf{J}}{n} + \frac{1}{2}u^2 D, \\
\frac{1}{\Gamma - 1}\left(\frac{\partial p_e}{\partial t} + \nabla\cdot p_e\mathbf{u}\right) &= -p_e\nabla\cdot\mathbf{u} + \frac{d_i}{\Gamma - 1}\frac{\mathbf{J}}{n}\cdot\left(\nabla p_e - \Gamma\frac{p_e}{n}\nabla n\right) \\
&\quad - \nabla\cdot\mathbf{q}_e + d_i\Pi_e : \nabla\frac{\mathbf{J}}{n}, \\
\frac{\partial \mathbf{B}}{\partial t} &= -\nabla\times\mathbf{E}, \\
\mathbf{J} &= \nabla\times\mathbf{B}, \\
\mathbf{E} + \mathbf{u}\times\mathbf{B} &= \frac{d_i}{n}\left(\mathbf{J}\times\mathbf{B} - \nabla p_e - \nabla\cdot\Pi_e + \mathbf{R} + \mathbf{F}\right).
\end{aligned}
$$

M3D-C^1: What's New

Improvements to M3D-C^1since last published results:

- Numerical integration (79-point Gaussian quadrature).
- Unstructured mesh
- Option for toroidal geometry
- Integration with PETSc
- Different implicitization and time integration schemes (semi-implicit, fully implicit; Crank-Nicholson, BDF2).

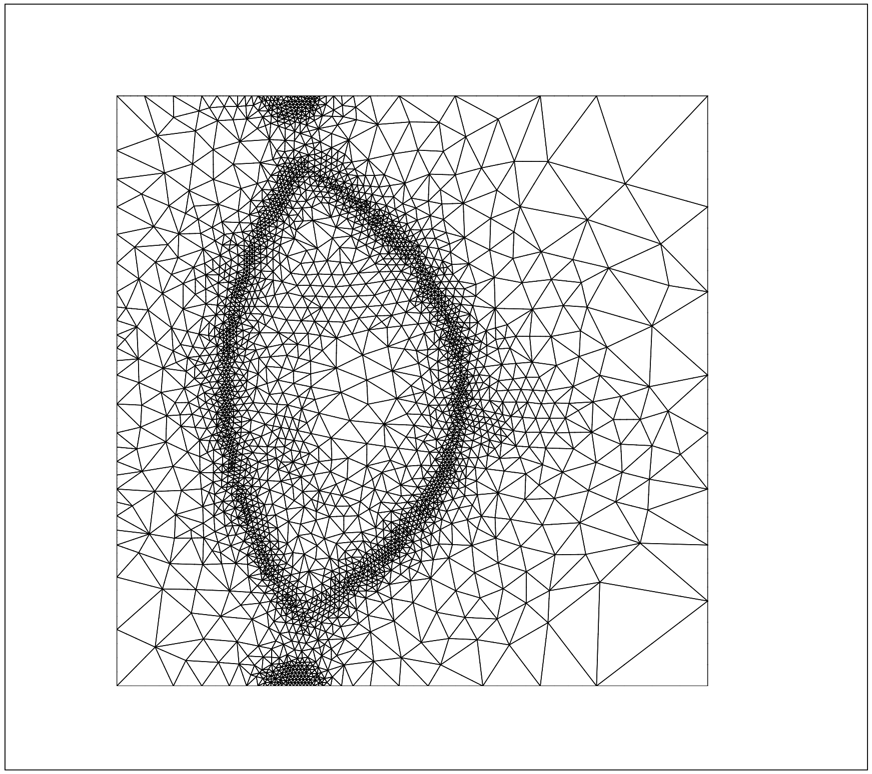

M3D-C^1: Implicitization issues

- Published results from M3D-C^1 used a split time step, where velocity advance looked like:

$$[1 - \theta^2(\delta t)^2 \mathcal{L}]u^{n+1} = [1 - \theta(\theta - 1)(\delta t)^2 \mathcal{L}]u^n + \delta t c \nabla v^n$$

- In toroidal simulations in which the flow is driven by resistivity, our results converged very slowly with δt.
  - We implemented a fully implicit, unsplit time step as a check on our results. This showed that the split time step method was introducting significant errors even at small values of δt.
  - By letting $\theta(\theta - 1) \to \theta^2$, as done by Caramana [5] and NIMROD, these errors were elimintated.

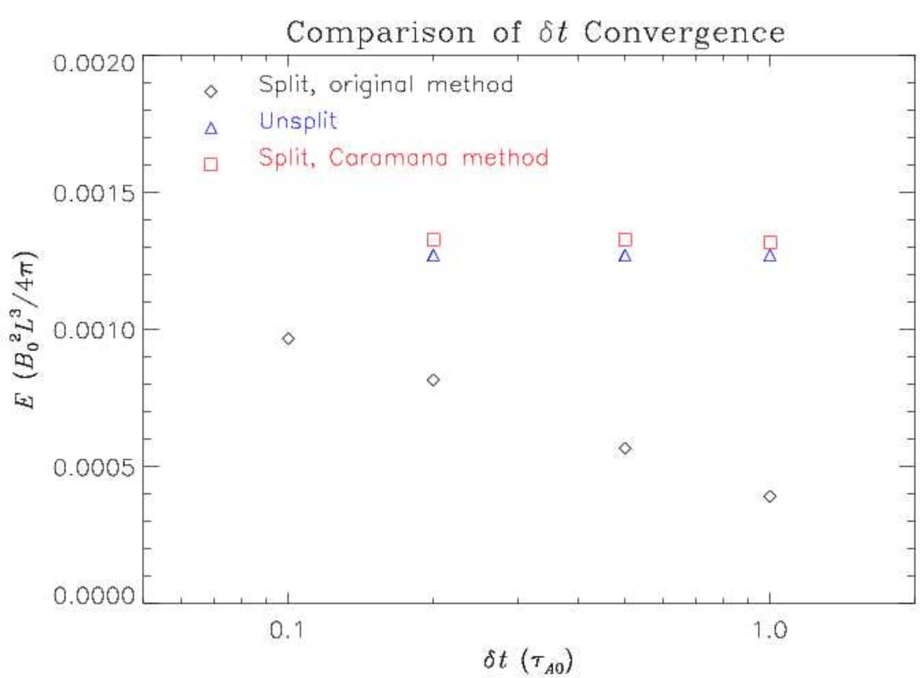

Results: Toroidal Steady States

The following data result from simulations of the following scenario:

- The simulation is initialized with a solution to the Grad-Shafranov equation.
- A loop voltage is applied by changing the flux at the boundary of the simulation domain at a constant rate $\dot{\psi} = V_L/2\pi$.
- The simulation is run until a steady state in both current profile and flow is reached.
- The resistivity is proportional to $T^{-3/2}$. The vacuum region is simply a low temperature region outside the separatrix.
- A localized density source in included to offset diffusive flux out of the simulation domain.
- Viscosity smoothly becomes vary large at the boundary to damp flows in the vacuum region.

Results: Toroidal Steady States

Hydrodynamic profiles relax to a true steady-state. Here are the initial and steady-state profiles for a simulation of an NSTX-like profile ($a/R \approx 1$, $\beta \approx 15\%$):

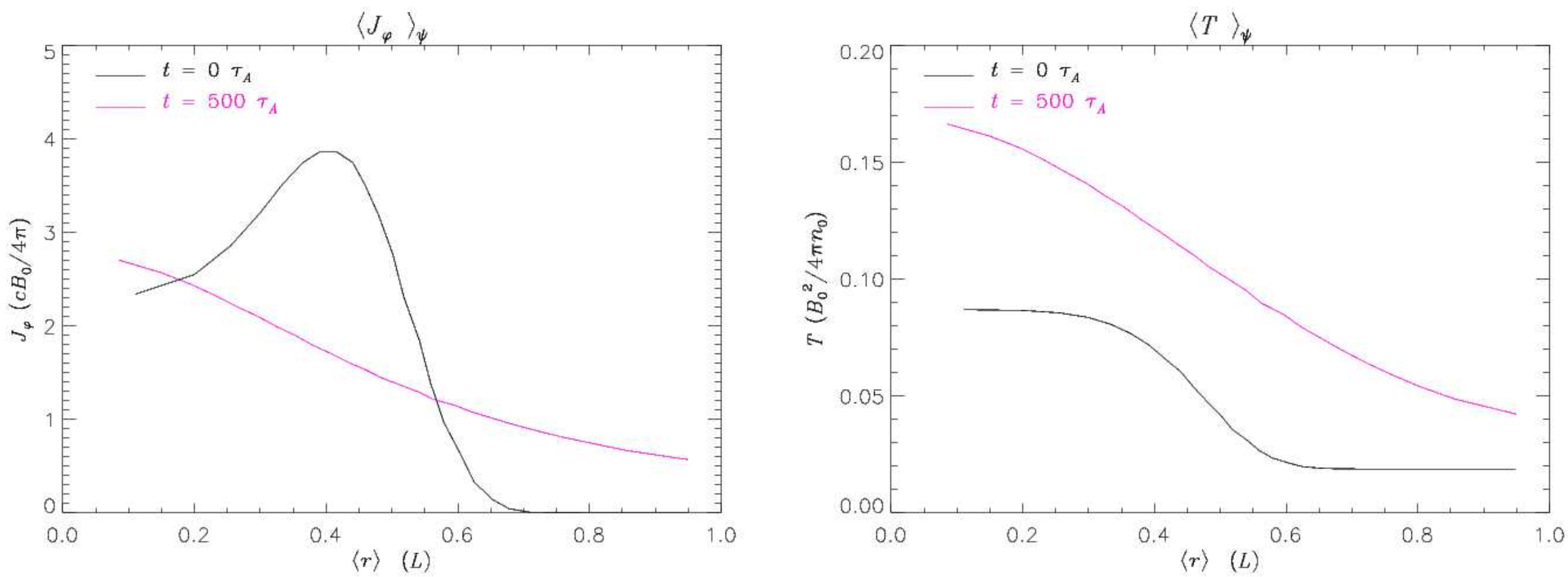

Results: Comparison with Theory

- The current implementation of gyroviscosity has been tested successfully against the previous (published) implementation that used analytic integrations. M3D-C^1 with GV also was able to reproduce linear eigenvalues of MRI in toroidal geometry accurately.

- Simulation results agree relatively well with one-dimensional analytic predictions of the cross-surface (Pfirsch-Schlüter) flow.

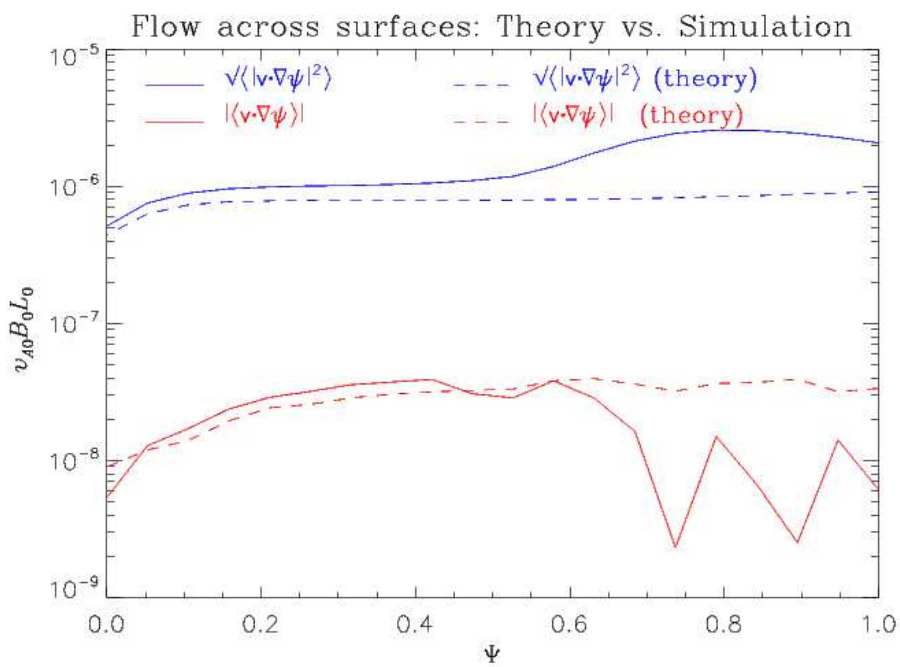

Results: Spontaneous Rotation

- It was predicted by Stringer [6] that non-rotating toroidal equilibrium should be unstable in resistive-MHD.
- Simulations of a large-aspect ratio, low-β plasma confirm that this happens when density diffusion is not too high.
- These simulations are run with the following parameters:

$$
\begin{aligned}
B_T/B_p &\approx 200 & q &\approx 3 \\
\beta &\approx 2\times 10^{-4} & S &\sim 10^5 \\
a/R &\approx 1/20 & Re &\sim 10^8 \\
\kappa &= 10^{-5} n_0 L^2/\tau_A & \kappa_\parallel &= n_0 L^2/\tau_A
\end{aligned}
$$

Results: Spontaneous Rotation

Poloidal rotation is found to occur spontaneously at sufficiently low rates of density diffusion.

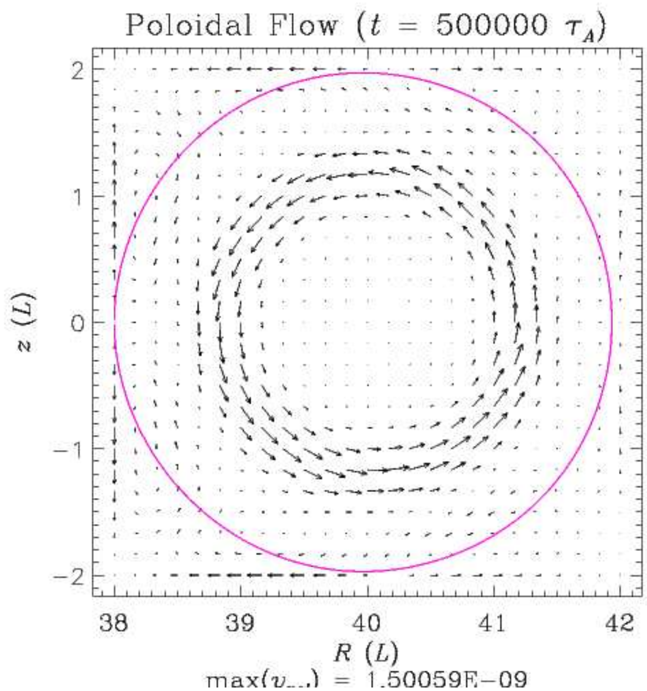

$$D = 10^{-5} L^2/\tau_A$$

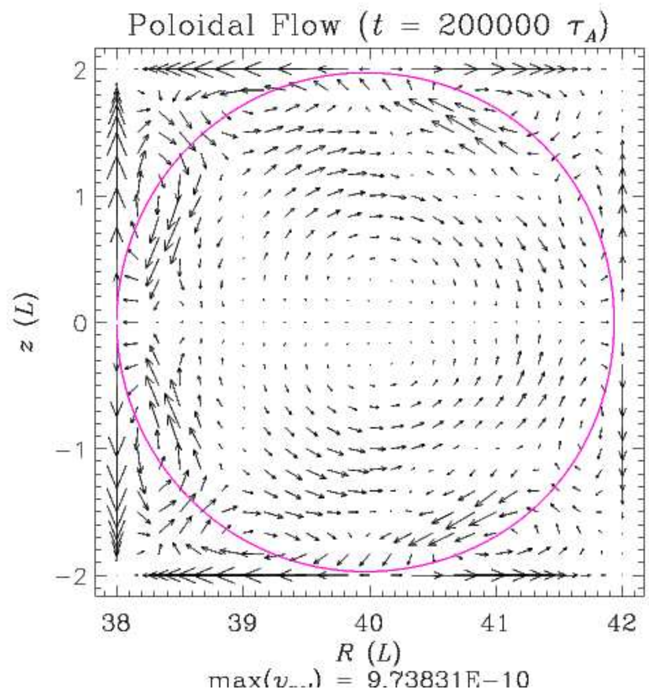

$$D = 10^{-3} L^2/\tau_A$$

Results: Rotation due to gyrovsiscosity

- We have not observed spontaneous rotation in resistive- or Hall-MHD simulations of NSTX-like plasmas (high-β, low aspect-ratio, elongated, and diverted), without gyroviscosity.
- Including gyroviscosity leads to significant rotation in NSTX-like plasmas.
- In the large aspect-ratio simulations, gyroviscosity has virtually no effect.
- We do not fully understand the physics of this spin-up yet.
- These simulations use NSTX coil configurations with the following parameters:

$$B_T/B_p \approx 3 \qquad q \approx 1$$

$$\beta \approx 15\% \qquad S \sim 10^3$$

$$a/R \approx 1 \qquad Re \sim 10^5$$

$$\kappa = 2 \times 10^{-2} n_0 L^2/\tau_A \qquad \kappa_\parallel = 75 n_0 L^2/\tau_A$$

Results: Toroidal Velocity

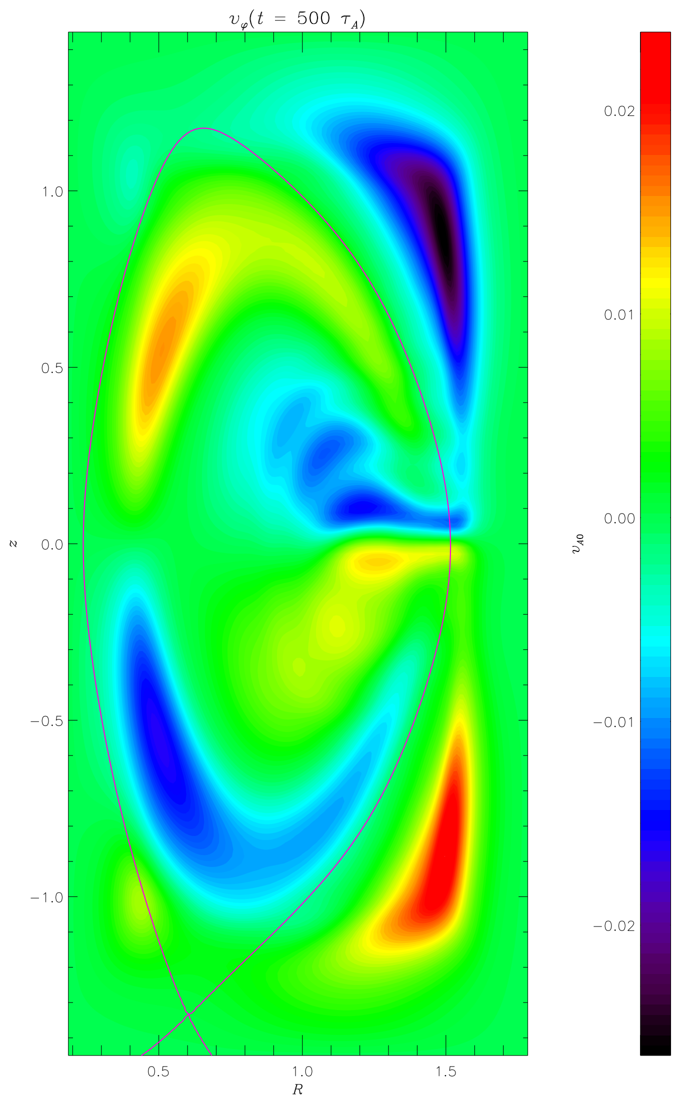

Without gyroviscosity

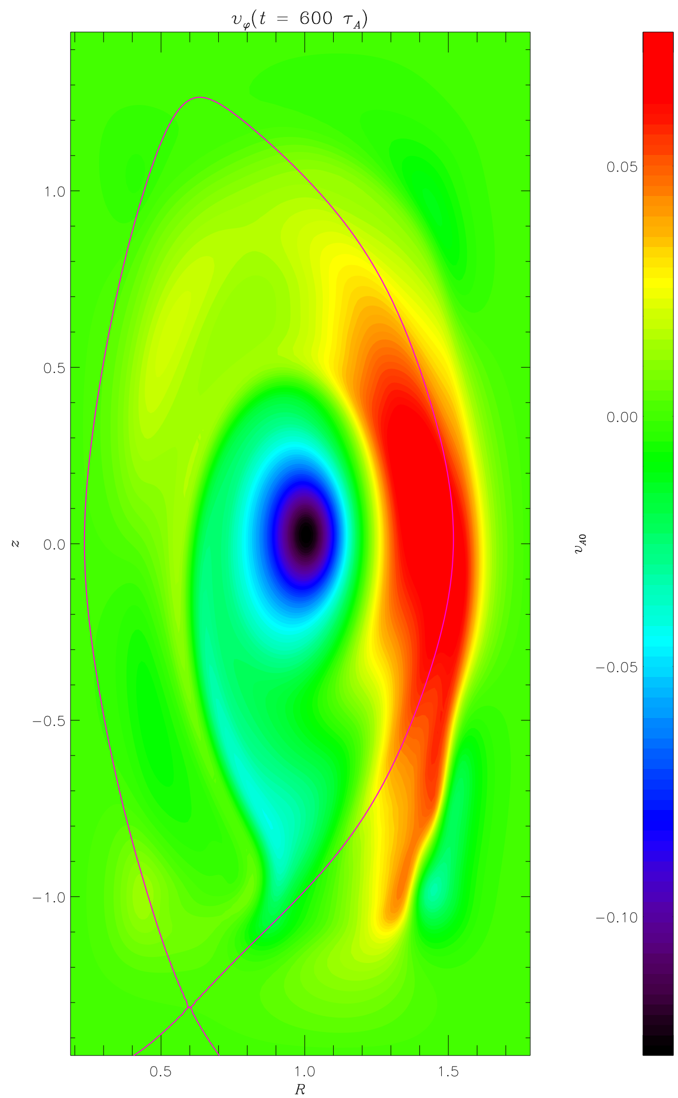

With gyroviscosity

Results: Poloidal Velocity

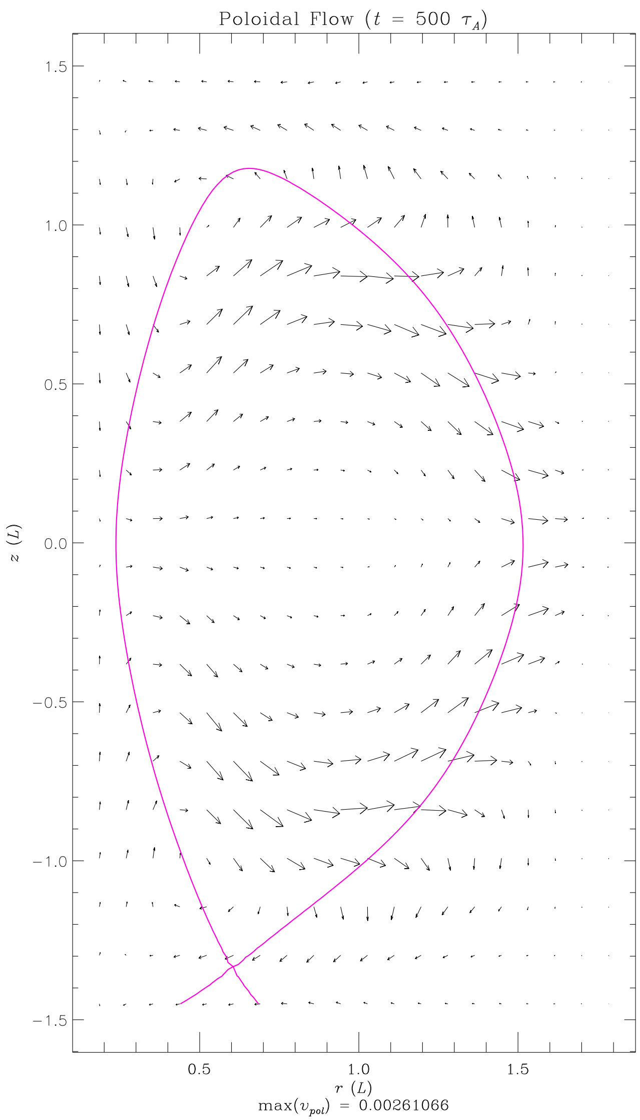

Without gyroviscosity

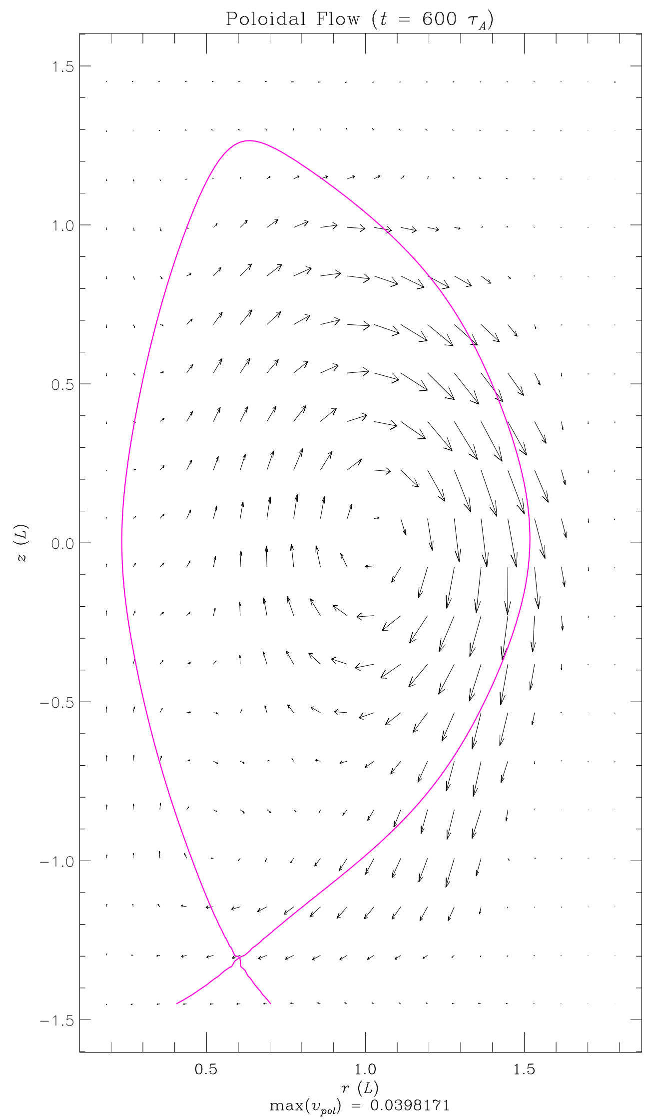

With gyroviscosity

Conclusions

- We have been able to obtain self-consistent steady-states of the extended-MHD equations for realistic plasma configurations with free boundaries.
- The flows observed in the simulations are in relatively good agreement with one-dimensional theoretical predictions.
- Spontaneous poloidal rotation has been observed to occur in large aspect-ratio, circular cross-section configurations, as has been predicted.
- Gyroviscosity leads to plasma rotation in NSTX-like configurations.

Future Work

- We are working to gain an analytical understanding of the spin-up due to gyroviscosity.
- We are also working to simulate H-mode profiles, to observe the self-consistent flows in the presence of an edge pedestal.
- These steady-states will serve as a starting point for three-dimensional linear stability calculations. Work to extend M3D-C^1 to do 3D linear stability calculations is beginning.
- We plan to develop M3D-C^1 into a fully three-dimensional implicit nonlinear code.

References

[1] S. C. Jardin and J. A. Breslau, Phys. Plasmas **12**, 056101 (2005).

[2] S. C. Jardin, J. Comp. Phys. **200**, 133 (2004).

[3] X. S. Li and J. W. Demmel, ACM Trans. Mathematical Software **29**, 110 (2003).

[4] S. I. Braginskii, in *Reviews of Plasma Physics*, edited by M. A. Leontovich (Consultants Bureau, New York, 1965), vol. 1, pp. 205–311.

[5] E. J. Caramana, J. Comp. Phys. **96**, 484 (1991).

[6] T. E. Stringer, Phys. Rev. Lett **22**, 770 (1969).